www.amlett.com, www.vbripress.com/aml, DOI: 10.5185/amlett.2015.5884 Published online by the VBRI Press in 2015

Single oriented CeO_2 buffer layer deposition on biaxially textured Ni-W substrate by RF magnetron sputtering

K. M. K. Srivatsa, Preetam Singh*, Sourav Das

Physics of Energy Harvesting Division, Council of Scientific & Industrial Research (CSIR) - National Physical Laboratory, Dr. K.S. Krishnan Marg, New Delhi 110012, India

*Corresponding author. Tel: (+91) 1145608609; E-mail: singhp@mail.nplindia.org

Received: 04 March 2015, Revised: 05 March 2015 and Accepted: 19 June 2015

ABSTRACT

Considerable attention has been gained on the deposition of CeO_2 thin films with (200) single orientation as hetero-epitaxial buffer layer on (200) oriented biaxially textured flexible Ni substrates, in the fabrication of superconductor and semiconducting epitaxial thin films for device applications. In this work we have deposited (200) oriented CeO_2 thin films on biaxially textured Ni-W substrate in a single-step process by RF magnetron sputtering, using CeO_2 target. X-ray diffraction analysis shows that for the CeO_2 thin film deposited at RF sputtering power below 200 W and for the substrate temperature of 700 ^oC, the film assumes single (200) orientation. For the substrate temperature below 700 ^oC and RF sputtering powers above 200 W the film shows polycrystalline nature with (111) and (200) orientations. The Raman spectrum of single oriented (200) CeO_2 thin film shows only one sharp peak at about 464 cm^{-1} corresponds to the presence of F_{2g} mode of CeO_2. The ellipsometry studies reveal the value refractive index and optical band gap of single oriented film as 2.52 and 3.41 eV, respectively. Copyright © 2015 VBRI Press.

Keywords: CeO_2 buffer layer; RF magnetron sputtering; XRD; Raman spectrum; optical properties.

Introduction

In the recent years efforts are being put to fabricate high-Tc superconducting (HTS) wire and semiconductor thin film based solar cells on biaxially textured flexible single oriented Ni substrates, owing to its obvious advantages [**1-6**]. Normally a buffer layer is used in order to prevent the reaction between the Ni substrate and the superconductor/ semiconducting films during their high temperature processing, and also to demonstrate a lattice match to both the substrate and film so that epitaxial growth may be maintained. There are different kinds of buffer layers that are of research interest on biaxially textured Ni substrate such as YSZ, Y_2O_3, $La_2Zr_2O_7$, $SrTiO_3$, $LaMnO_3$ and CeO_2 [**7-13**]. Among these buffer layers CeO_2 has a good structural compatibility with YBCO superconductor (~ 0.62% lattice mismatch) and Si (< 0.1% lattice mismatch) and also has an excellent thermal and chemical stability with Ni, and thus serves as a good buffer layer [**3, 13, 14**]. Further, as the cubic textured Ni substrate has (200) crystallographic orientation, the preferred orientation of deposited CeO_2 buffer has to be the same (200) orientation in order to grow epitaxial layers over it. In practice, for practical applications about 60-100 nm thick CeO_2 films are used as single buffer layer or as one of the layers in the multilayered buffer stake [**4**]. Typically, deposition of metal oxide films occurs at high temperatures, which lead to formation of NiO unfavorably on the surface of Ni substrates preventing the epitaxial growth. Thus it is necessary to avoid the formation of NiO.

Many workers have reported deposition of CeO_2 with (200) orientation following several techniques and involving single-step and/or multi-step processes using seed layer and high temperatures etc. Wang *et al.* [**15**] reported the deposition of CeO_2 films with (200) orientation by ion beam assisted pulsed laser deposition (PLD) on Ni (001) substrate. Paranthaman *et al.* [**12**] have grown, epitaxial films of CeO_2 using a metal-organic deposition (MOD) process. Recently, Lee *et al.* [**16**] have developed a two-step deposition of CeO_2 thin films on biaxially textured Ni substrate by E-beam evaporation and observed (200) orientation by inserting a thin CeO_2 seed layer of 10 nm thickness under slow deposition rate in first step and then homo-epitaxial layer at high deposition rate in second step. Among various thin film deposition techniques RF/DC magnetron sputtering has been recognized as a promising versatile technique for the deposition of stoichiometric films of metal oxides. Its main advantage is good adhesion to substrates, and high density and homogeneity of deposited films. Moreover it permits large scale deposition of high quality films at high deposition rates. Xiong et al. [**17**] reported the deposition of (200) oriented CeO_2 films in two steps by depositing Ce metal by DC magnetron sputtering followed by oxidation under forming gas

(96%Ar + 4%H_2) ambient in order to avoid the formation of NiO. Similarly, Wee *et al.* [**4**] have deposited (200) oriented CeO_2 by reactive sputtering, to use it in a buffer stake for the fabrication of heteroepitaxial Si film for solar cell. Not much details are available on the deposition of CeO_2 films with (200) orientation on Ni substrates by RF magnetron sputtering. Wang *et al.* [**18**] reported the deposition of polycrystalline CeO_2 films by RF magnetron sputtering in two steps, first deposing the seed layer in forming gas followed by deposition under Ar + O ambient. It is highly desirable that the deposition of single oriented CeO_2 films should be deposited in a single step process on Ni substrates, avoiding the formation of NiO in order to grow superconducting and semiconducting epitaxial layers for device applications.

In our present work we have made an attempt to deposit CeO_2 thin films by RF magnetron sputtering technique and observed single (200) orientation in a single step without the formation of NiO, and characterized the deposited films for its structural and optical properties, and the results are presented.

Experimental

Material synthesis

For this study, we have procured biaxially textured and (200) oriented Ni-5at% W (Ni-W) substrates, having large grains in the range 50-100 µm, from the manufacturer M/s Evico GmbH, Germany. CeO_2 thin films have been deposited using CeO_2 target (99.99%, China Rare Metal Material, China) in an in-house designed and fabricated downstream RF magnetron sputtering system. A turbo-based pumping system backed by roots and rotary pumps was used to achieve a base pressure about 1×10^{-6} Torr. High-purity Ar (99.999%, BOC, India) was used as sputtering gas. The deposition pressure in the vacuum chamber was measured by a compact process ion gauge (Pfeiffer) and the gas flow rate (15 sccm) was accurately controlled by mass flow controllers (Aalborg, model: GFC-17). The sputtering pressure and distance between the sputtering target and substrate were kept fixed at 30 m Torr and 3 inches, respectively. The depositions were carried out at various sputtering powers in the range 100-300 W and also at different substrate temperatures varying from 600 ^{o}C to 700 ^{o}C. The deposition time was also varied to deposit CeO_2 films of different thicknesses.

Characterizations

The structural properties of CeO_2 thin films were characterized by an X-ray diffractometer (Bruker, Germany, model: D8-Avalance), using Cu Kα radiation at 1.54 Å in θ-2θ geometry. The structural properties were also evaluated at room temperature by Raman Spectrometer (InVia Renishaw) using 514 nm Ar ion laser as the excitation source with 5 mW power. The optical properties of CeO_2 thin films were investigated by Spectroscopic ellipsometer (J. A. Woollam, model: VASE32) and the optical parameters were calculated in the wavelength range 250-1100 nm, for the incident angles of 65^{o} and 75^{o}. The surface morphology was examined by a Scanning electron microscope (SEM, model: LEO 400).

Results and discussion

Fig. 1 shows the XRD pattern of CeO_2 thin films deposited at different RF sputtering powers varying from 100 W to 300 W, while the substrate temperature and deposition pressure were tentatively selected and kept constant at 700 ^{o}C, 30 m Torr respectively and also the thickness of the film kept within 100 nm. At 100 W sputtering power single (200) orientation of CeO_2 peak was observed but with poor crystallinity. As the sputtering power increased to 150 W, the intensity of (200) peak increased but with another very low intensity (111) peak has been observed. At 200 W sputtering power only a single high intensity and sharp (200) peak has been observed. Further, increase in sputtering power to 300 W resulted polycrystalline CeO_2 film with (111) and (200) orientations. The increased RF sputtering power increases the sputter rate, thereby, increase in the deposition rate. In our present work it appears that the deposition rate about 1.2 Å /sec, at the RF power of 200 W along with the substrate temperature 700 ^{o}C, favored to result in single (200) oriented CeO_2 film. It is to be noted that, no traceable peak related to NiO has been observed in our studies. It is understandable here that, if the applied RF power does not crack the sputtered CeO_2 molecules into Ce and O, then the possibility for the formation of NiO can be avoided.

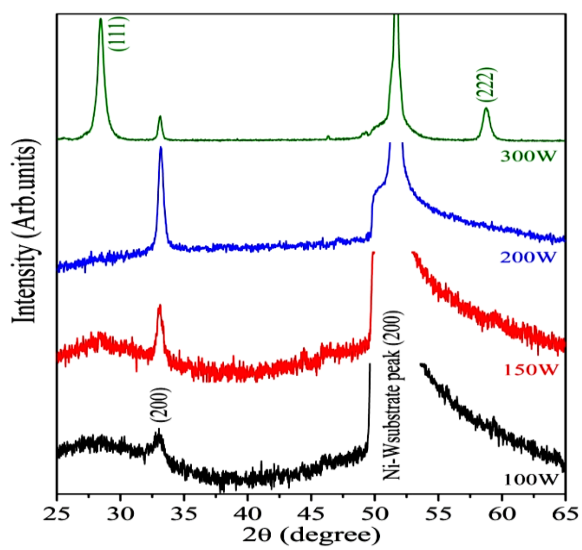

Fig. 1. X-ray diffraction pattern of CeO_2 thin films deposited on biaxially textured Ni-W substrate at different applied RF sputtering powers.

Fig. 2 shows the XRD pattern of CeO_2 thin films deposited at different substrate temperatures varying from 600 ^{o}C to 700 ^{o}C while the sputtering power and deposition pressure were kept fixed at 200 W and 30 m Torr, respectively. The film deposited at 600 ^{o}C shows mixed orientations with almost same intensity of (111) and (200) peaks. When the substrate temperature increased to 650 ^{o}C, the intensity of (200) peak gradually increased further while the intensity of (111) peak decreased and at 700 ^{o}C a single dominant (200) oriented peak appeared. This shows that substrate temperature 700 ^{o}C is in favor to the diffusion of atoms absorbed on the substrate and accelerates the migration of atoms to the energy favorable positions, resulting in the enhancement of the crystallinity and follows the crystal structure and orientation that of the Ni substrate [**19**]. The depositions were also carried out by varying the deposition time in order to investigate the effect of film thickness on the structure of deposited films, at the optimized values of sputtering power (200 W), substrate temperature (700 ^oC) and the deposition pressure (30 mTorr), that is, keeping the growth rate constant. It has been observed that the films above 100 nm thick show the polycrystalline nature with both (111) and (200) orientations.

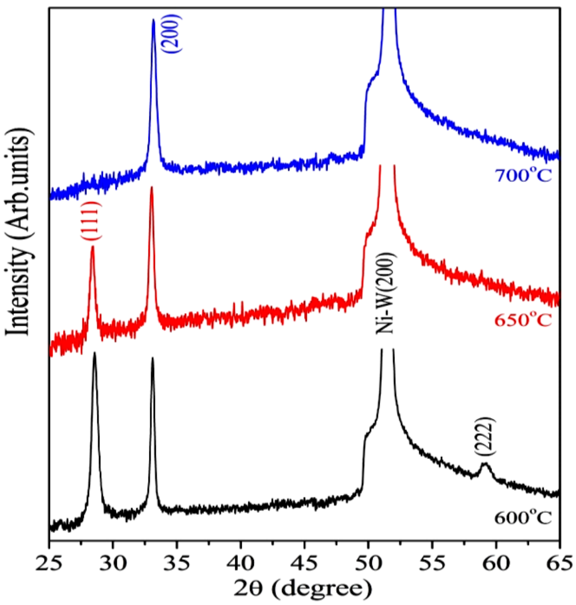

Fig. 2. X-ray diffraction pattern of CeO_2 thin films deposited on biaxially textured Ni-W substrate at different substrate temperatures.

Raman spectrum for the CeO_2 thin film, deposited at the optimized process parameters to obtain a single (200) orientation, has been recorded at room temperature and is shown in **Fig. 3**.

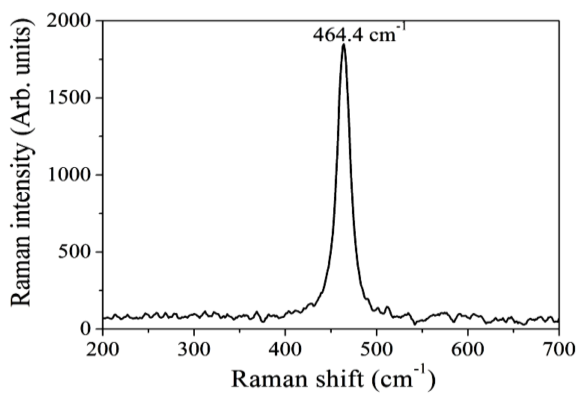

Fig. 3. Raman spectrum of CeO_2 thin film deposited at 700 ^oC and 200 W substrate temperature and RF sputtering power, respectively.

The spectrum shows a sharp intense peak at about 464 cm^{-1}, corresponding to F_{2g} Raman mode of CeO_2, which indicates the formation of highly crystalline CeO_2 thin film [**20, 21**]. Generally, the metal oxides with fluorite structure such as CeO_2 have only a single allowed Raman F_{2g} mode. This mode represents a symmetric breathing mode of oxygen atoms around each cation. The oxygen atom moves in this mode and its frequency is nearly independent on cation's mass. McBride *et al.* [**20**] reported that the Raman peak at 570 cm^{-1} is due to the oxygen vacancies. On the other hand Anwar et al. [**21**] observed a defect peak at 565 cm^{-1}, which corresponds to disorder in the oxygen sub-lattice (oxygen vacancies). They have reported that these defect peaks correspond to disorder in oxygen sub-lattice more in the film deposited at room temperature and nanocrystalline size. We have not observed any such peak arising due to defects / oxygen vacancies in our case and hence confirm the high quality defect free CeO_2 thin film.

The optical properties of CeO_2 thin film with (200) orientation, were studied by Spectroscopic ellipsometer (SE) in the wavelength range 250-1100 nm. SE measurements provide the data related to the ellipsometer angle Ψ and phase Δ with respect to the wavelength or energy. Ellipsometer is a model fitting based technique, which minimizes the difference between measured experimental and calculated fitting values as a function of wavelength or photon energy [**22**]. **Fig. 4** represents the SE data for the ellipsometric parameters (Ψ and Δ) of CeO_2 thin film deposited at the optimized deposition parameters. The solid line in the figures represents the model-fits data and it can be seen that all the features present in the experimental spectra are well matched with the model fits. The fitting parameters within the parametric dispersion model yields thickness of deposited CeO_2 thin film about 80±0.5 nm which is in good agreement with the thickness of 82±1.0 nm measured by stylus profiler.

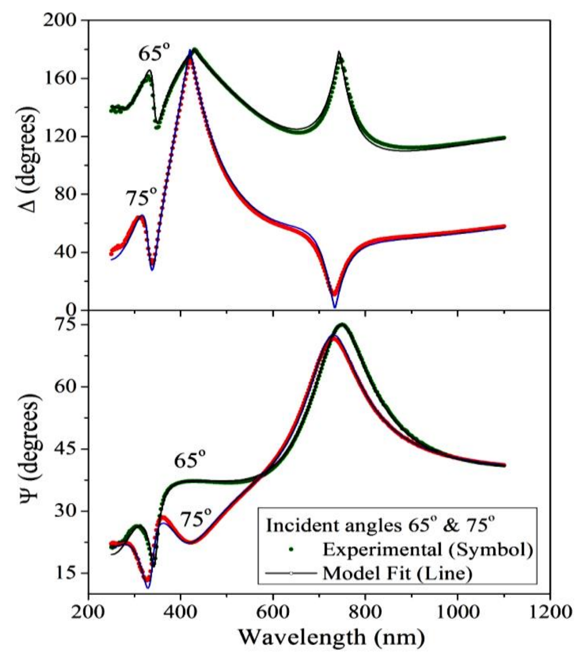

Fig. 4. Experimental and model fitted ellipsometric parameters (Ψ & Δ) of CeO_2 thin film deposited at 700 ^oC and 200 W substrate temperature and RF sputtering power, respectively. Solid line indicates model fit.

Fig. 5 represents the refractive index (n) and extinction coefficient (k) as a function of wavelength in the range 250-1100 nm, as obtained from the corresponding ellipsometric data. The value of refractive index at 600 nm wavelength was found as 2.52. Optical band gap (E_g) of the film can be calculated using the well-known Tauc relation based on inter-band absorption theory [**23**]. The absorption coefficient (α) is extracted from the ellipsometric data after the model fit and the indirect band gap of the CeO_2 film was evaluated by extrapolating the straight line part of the curve $(ahv)^{1/2} = 0$ as shown in the inset of **Fig. 5**. So the calculated value of optical band gap is 3.41 eV for the CeO_2 thin film deposited at the optimized deposition conditions. The observed values of n and E_g are also in good agreement with the previously reported results of highly oriented crystalline CeO_2 thin film deposited by other techniques on Si substrate, and the values of single crystal [**24, 25**]. No such report is available on the optical properties of CeO_2 thin films deposited over biaxially textured flexible Ni substrate. The scanning electron microscope (SEM) images (with low and high magnifications) in **Fig. 6** show the surface morphology of CeO_2 thin film grown at the optimized deposition parameters. Crack free surface with large sized grains of CeO_2 film, and well separated by grain boundaries (GBs), can be seen clearly in the micrograph. It is observed that most of the grains are having the size of tens of microns, following the texture of Ni-W substrate.

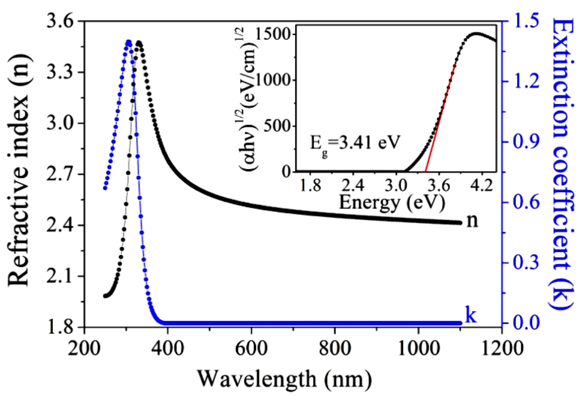

Fig. 5. Dispersion behavior of refractive index (n) and extinction coefficient (k) of CeO_2 thin film deposited 700 °C and 200 W substrate temperature and RF sputtering power, respectively. Inset shows vs hv plot of the same sample.

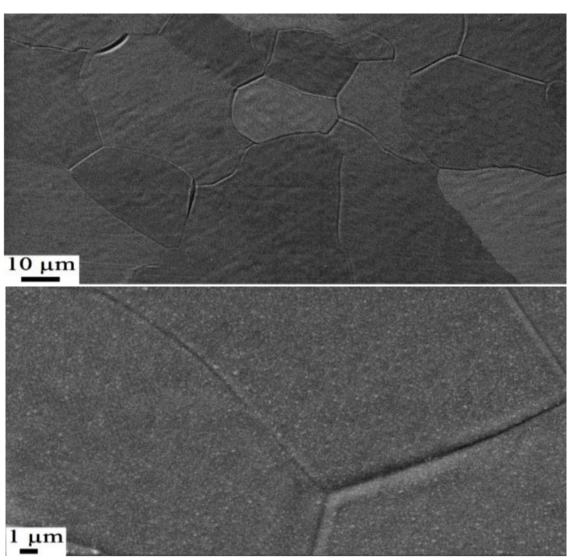

Fig. 6. SEM images with low and high magnifications of CeO_2 thin film deposited at 700 °C and 200 W substrate temperature and RF sputtering power, respectively.

Conclusion

In conclusion, we have successfully deposited single oriented CeO_2 buffer layer on biaxially textured flexible Ni-W substrate in single step by RF magnetron sputtering technique using CeO_2 ceramic target. The XRD pattern confirms formation of (200) orientation for 80 nm thick CeO_2 film deposited at 700 °C and 200 W substrate temperature and RF sputtering power, with no formation of NiO at the interface. For the optimized CeO_2 thin films we have also achieved the value of refractive index (2.52) and optical band gap (3.41 eV) close to that of standard values. SEM images show the micro-crack free micron size grains and Raman spectrum confirms the defect free CeO_2 film. It has been observed that the RF sputtering power, substrate temperature and the film thickness play a key role in the formation of (200) single orientation. These (200) oriented CeO_2 buffer layer are of interest in the fabrication of superconductor and semiconducting epitaxial films on biaxially textured flexible Ni substrates, for device applications.

Acknowledgements

The authors are grateful to the Director, CSIR-National Physical Laboratory, for his continuous encouragement and support during this work. Authors would like to fully acknowledge the help of Dr. V.P.S. Awana, Dr. B.P. Singh and Mr. K.N. Sood for XRD Raman and SEM measurements, respectively.

Author contributions

Conceived the plan: KMKS, PS; Performed the expeirments: PS, SD; Data analysis: KMKS, PS, SD; Wrote the paper: KMKS, PS. Authors have no competing financial interests

Reference

1. Engel, S.; Knoth, K.; Huhne, R.; Schultz, L.; Holzapfel, B. *Supercond. Sci. Technol*., **2005**, *18*, 1385.
   DOI: 10.1088/0953-2048/18/10/024
2. Solovyov, VF.; Develos-Bagarinao, K.; Li, Q.; Qing, J.; Zhou, J. *Supercond. Sci. Technol*. **2010**, *23*, 014008.
   DOI: 10.1088/0953-2048/23/1/014008
3. Xiong, J.; Chen, Y.; Qiu, Y.; Tao, B.; Qin, W.; Cui,Tang, J.; X.; Li, Y. *Supercond. Sci. Technol*., **2006**, *19*, 1068.
   DOI: 10.1088/0953-2048/19/10/014
4. Wee, SH.; Cantoni, C.; Fanning, TR.; Teplin, CW.; Bogorin, DF.; Bornstein, J.; Bowers, K.; Schroeter, P.; Hasoon, F.; Branz, HM.; Paranthaman, MP.; Goyal, A.; *Energy Environ. Sci.*, **2012**, *5*, 6052.
   DOI: 10.1039/C2EE03350J
5. Singh, P.; Srivatsa, KMK.; Das, S.; *Adv. Mater. Lett*., **2015**.
   DOI: 10.5185/amlett.2015.5754
6. Dutta, P.; Rathi, M.; Yao, Y.; Gao, Y.; Majkic, G.; Iliev, M.; Martinez, J.; Holzapfel, B.; Selvamanickam, V. *RSC Adv*., **2014**, *4*, 21042.
   DOI: 10.1039/C4RA02664K
7. Chen, J.; Parilla, PA.; Bhattacharya, RN.; Ren, ZF. *Jpn. J. Appl. Phys*., **2004**, *43*, 6040.
   DOI: 10.1143/JJAP.43.6040
8. Park, C.; Norton, DP.; Lee, DF.; Verebelyi, DT.; Goyal, A.; Christen, DK.; Budai JD. *Physica C*., **2000**, 341–348, 2481.
   DOI: 10.1016/S0921-4534(00)01199-0
9. Shi, DQ.; Ko, RK.; Song, KJ.; Chung, JK.; Ha, HS.; Kim, HS.; Moon, SH.; Yoo, SI.; Park, C. *Supercond. Sci. Technol*., **2005**, *18*, 561.
   DOI: 10.1088/0953-2048/18/4/029
10. Cheng, YL.; Suo, HL.; Zhao, Y.; Gao, MM.; Zhu, YH.; Wang, R.; Liu, M.; Ma, L.; Zhou, ML. *Physica C*., **2011**, *471*, 982.
    DOI: 10.1016/j.physc.2011.05.105
11. Aytug, T.; Paranthaman, M.; Kang, S.; Zhai, HY.; Leonard, KJ.; Vallet, CE.; Sathyamurthy, S.; Christen, HM.; Goyal A.; Christen, DK. *IEEE Trans. Appl. Supercond*., **2003**, *13*, 2661.
    DOI: 10.1109/TASC.2003.811942

12. Paranthaman, MP.; Qiu, X.; List, FA.; Kim, K.; Zhang, Y.; Li, X.; Sathyamurthy, S.; Thieme, C.; Rupich, MW. *IEEE Trans. Appl. Supercond*. **2011**, *21*, 3059.
DOI: 10.1109/TASC.2010.2092731
13. Zhao, Y.; Grivel, J-C. *CrystEngComm*, **2013**, *15*, 3816.
DOI: 10.1039/c3ce40245b
14. Lee, H-G.; Lee, Y-M.; Shin, H-S.; Kim C-J.; Hong, G-W. *Mater. Sci. Eng. B*. **2002**, *90*, 20.
DOI: 10.1016/S0921-5107(01)00940-0
15. Wang, RP.; Zhou, YL.; Pan, SH.; He, M.; Lu, HB.; Chen, ZH.; Yang, GZ.; Liu, CF.; Wu, X.; Wang, FY.; Feng, Y.; Zhang, PX.; Wu, XZ.; Zhou, L. *Physica C*. **2000**, *337*, 87.
DOI: 10.1016/S0921-4534(00)00062-9
16. Lee, JB.; Park, SK.; Kim, BJ.; Lee, HJ.; Kim, SS.; Moon, SH.; Lee HG.; Hong, GW. *Physica C*. **2011**, *471*, 978.
DOI: 10.1016/j.physc.2011.05.104
17. Xiong, J.; Chen, Y.; Qiu, Y.; Tao, B.; Qin, W.; Cui, X.; Li, Y. *J. Mater. Sci. Technol*. **2007**, *23*, 457.
URL: jmst.org/EN/Y2007/V23/I04/457
18. Wang, Y.; Xu, D.; Li, Y.; Liu, L. *Nano. Res. Lett*. **2013**, *8*, 304.
DOI: 10.1186/1556-276X-8-304
19. Singh, P.; Kumar, A.; Deepak, Kaur, D. *J. Cryst. Growth*. **2007**, *306*, 303.
DOI: 10.1016/j.jcrysgro.2007.05.023
20. McBride, JR.; Hass, KC.; Poindexter, BD.; Weber, WH. *J. Appl. Phys*., **1994**, *76*, 2435.
DOI: 10.1063/1.357593
21. Anwar, MS.; Kumar, S.; Ahmed, F.; Arshi, N.; Seo, YJ.; Lee, CG.; Koo, BH. *Current Appl. Phys*., **2011**, *11*, S301.
DOI: 10.1016/j.cap.2010.11.053
22. Herzinger, CM.; Johs, B.; McGahan, WA.; Woollam, JA.; Paulson, W.; *J. Appl. Phys*. **1998**, *83*, 3323.
DOI: 10.1063/1.367101
23. Tauc, J. (Ed.), *Amorphous and Liquid Semiconductor*, Plenium Press, New York, **1974**, *159*.
24. Balakrishnan, G.; Sundari, ST.; Kuppusami, P.; Mohan, PC.; Srinivasan, MP.; Mohandas, E.; Ganesan, V.; Sastikumar, D. *Thin Solid Films*. **2011**, *519*, 2520.
DOI: 10.1016/j.tsf.2010.12.013
25. Chiu, FC.; Lai, CM. *J. Phys. D: Appl. Phys*. **2010**, *43*, 075104.
DOI: 10.1088/0022-3727/43/7/075104